Small, high frequency probe for internal magnetic field measurements in high temperature plasmas

J. T. Slough[a)] and K. E. Miller
University of Washington, Redmond Plasma Physics Laboratory, 14700 NE 95th St., Redmond, Washington 98052

(Presented on 19 June 2000)

In previous experiments on high temperature (>50 eV), high density ($>10^{20}\,\mathrm{m}^{-3}$) plasmas such as the field-reversed configuration (FRC), it has not been possible to obtain direct information of the internal field structure in a nondestructive way. The probe surface would vaporize due to high electron thermal transport as well as ablate due to high energy ion bombardment. To minimize these processes, the smallest possible probes made from materials with the longest thermal time to melting were constructed and tested. In order to measure fast magnetic field changes (~several MHz), as well as not influence the FRC internal electric fields, the probe wall material was constructed from a nonconducting material. Of several insulating materials tested, beryllia was the only material that was found to be suitable. The probe wall consisted of a 0.3-m-long 2-mm-diam beryllia tube bored out to 1.5 mm. Inside the small bore, a ''chain'' probe of 24 loops was constructed out of 50-μm-diam magnet wire. The two axis probe measured axial and azimuthal FRC magnetic fields as small as a few gauss with centimeter resolution and a frequency response of 1 MHz or better. With the probe inserted, no changes in FRC confinement or behavior were observed over the entire 1 ms lifetime of the discharge. © *2001 American Institute of Physics.*
[DOI: 10.1063/1.1316752]

I. INTRODUCTION

In previous experiments on high temperature (>50 eV), high density ($>10^{20}\,\mathrm{m}^{-3}$) plasmas such as the field-reversed configuration (FRC), it has not been possible to obtain direct information on the internal field structure in a nondestructive way.[1,2] The reason for this was twofold: the probe surface would vaporize due to high plasma thermal loading as well as ablate due to high energy ion bombardment. Typically, after a few to several μs of exposure, the plasma impurity radiation from the probe would seriously alter the plasma confinement and structure.[3] In order to minimize these processes, the smallest possible probes made from materials with the longest thermal time to melting, τ_b, were constructed and tested. It was desired that the probe be capable of measuring fast magnetic field changes (up to several MHz), as well as not influence possible FRC internal electric fields. Both requirements dictated that the wall material be constructed from a nonconducting material. It was also desired that the probe should not have a significant influence on the plasma energy confinement time.

In designing the probe it was assumed that the probe would act as a thermal sink with the plasma flowing to the probe at the sonic speed and depositing all its energy there. Having this loss be a small fraction of the total energy lost from the plasma put an upper limit on the probe surface area that could be exposed to the plasma.

An estimate of the limiting probe size for the FRC can be obtained from a consideration of how plasma is lost from the FRC. For a FRC, the plasma is lost from the closed poloidal field volume into the open field line sheath at the outer separatrix radius r_s. This annular sheath has a characteristic width of the local ion gyroradius ρ_i.[4,5] The axial flow of plasma out of this sheath of area A_s ($\sim 2\pi r_s \rho_i$) is roughly sonic. The exposed probe area A_p for an internal probe that extends radially inward across the full radius of the FRC $\sim 2\pi r_p r_s$. For losses to the probe to be small, $A_p \ll A_s$, or equivalently the probe radius $r_p \ll \rho_i$. For the FRCs of interest ρ_i is typically ~1 cm.

II. MATERIALS SELECTION

The other constraint on the probe is that it be capable of absorbing the plasma energy without vaporizing during the discharge time. The relation between the incident power P on the probe surface, and the time τ_m required for the surface to reach the melting temperature T_m is given by[6]

$$\tau_m = \pi \kappa C \rho \left(\frac{T_m}{2P} \right)^2, \tag{1}$$

where κ is the thermal conductivity of the wall material, C is the specific heat, and ρ is the material density. A short list of possible probe wall materials is given in Table I. Several of these materials were tested in the TRAP FRC acceleration experiments.[7] FRCs at very high density ($5\times10^{21}\,\mathrm{m}^{-3}$), with temperatures $T_e = T_i = 110\,\mathrm{eV}$, were translated at high velocity ($v_t = 1.3\times10^5$ m/s) across small, hollow rods composed of various materials which were inserted and placed across the diameter of the vacuum tube, transverse to the axial FRC motion. The exposure time of the heat pulse to the rods was the transit time of the FRC across the rods, and for theses experiments ~10 μs. Given the high power density

[a)]Electronic mail: slough@aa.washington.edu

 © 2001 American Institute of Physics

Downloaded 18 Apr 2001 to 128.95.33.238. Redistribution subject to AIP copyright, see http://ojps.aip.org/rsio/rsicr.jsp

TABLE I. Physical characteristics of possible probe materials. The materials in bold were tested in the TRAP experiments.

	T_{melt} (K)	ρ (g/cm^3)	K (W/K/cm)	c (J/gK)	$10^{-6}T^2K\rho c$ surface response	τ_{melt} (μs) $P=50$ GW/m^2 (TRAP)
Tungsten	3700	19.0	1.80	0.13	60.9	1.911
Molybdenum	**2900**	**14.0**	**1.50**	**0.25**	**44.2**	**1.386**
Copper	1400	8.9	3.90	0.38	25.9	0.812
Platinum	2045	21.5	0.73	0.13	8.5	0.268
Aluminum	1000	2.8	2.40	0.90	6.0	0.190
Inconel	1700	8.2	0.30	0.20	1.4	0.045
Beryllium oxide	**2800**	**3.0**	**2.60**	**1.00**	**61.2**	**1.920**
Boron nitride	3300	2.2	1.80	0.71	30.6	0.961
Graphite	3600	2.0	1.50	0.50	19.4	0.610
Aluminum oxide	**2300**	**2.6**	**0.26**	**0.80**	**2.9**	**0.090**
Silicon oxide	**1900**	**2.6**	**0.02**	**0.74**	**0.1**	**0.003**

(50 GW/m^2), from the thermal as well as translational energy of the FRC intercepted by the rods, the melting time was much shorter than the transit time for all the materials tested. Surface changes could be observed on all the materials. The rise in rod temperature along the length of the material was recorded by a thermocouple after the discharge. The FRC radiation during the rod transit was monitored by a bolometer, and the FRC energy was measured by an axial array of excluded flux loops. Details of these measurements will be given elsewhere. The results can be summarized as follows. The final probe temperature was only 5%–10% of what would have been predicted from the full absorption of the plasma energy intercepted by the probe. It is assumed that the initial rapid vaporization led to a plasma cloud around the probe that reduced the subsequent power flow to the probe. Remarkably, even with the melting temperature exceeded, it was found that one of the materials tested, beryllia, caused no major degradation of the FRC energy confinement. With its superior thermal properties, once the surface had melted and produced the protective cloud, the reduced heat flow extended the time for further vaporization to a time greater than the FRC transit time, and no more erosion occurred.

The excluded axial flux, $\Delta\phi$, from the transit of the FRC was recorded by an array of magnetic loops along the axial length of the TRAP experiment. This signal is directly proportional to the internal FRC energy at the location of the loop.[1] The $\Delta\phi$ signal during FRC passage at locations upstream and downstream of the rod position is shown in Fig. 1. It can be seen that the usual probe materials, alumina and fused silica (quartz), caused rapid energy decay in the FRC, but that the FRC energy after transiting over the beryllia was essentially unchanged from when there was no rod. The impact of the vaporization of probe material was observed, however, in the radiated power observed by a bolometer mounted at the same axial location as the rods. There was a significant increase in radiated power for even the beryllia. This is no doubt due to the oxygen impurity from the beryllia. Since the oxygen is first in the lowest ionization state, it would be expected to radiate heavily until it was stripped down to the O^{+6} state for the $T_e \sim 100$ eV in these experiments.

Other materials may also show the same good behavior as beryllia, such as boron nitride or silicon nitride, but it was not possible to find a source that could fabricate these materials into a small radius rod, let alone a long hollow tube.

III. PROBE DESIGN

Suitably small tubes of beryllia with outer diameters of 2 mm in lengths up to 0.5 m were obtained from Brush Wellman. Fabrication constraints, however, limited the inner bore diameter to 0.9 mm. The tube's small bore presented a problem in that to measure magnetic fields as small as a few gauss with cm resolution, a large loop area was needed. Therefore the beryllia tube inner bore was incrementally bored out using very long diamond tipped drill bits to a diameter of 1.5 mm. To improve the effective loop area, several loop turns were employed for each B-dot probe. Since there was little room for a winding structure inside the small bore, a ''chain'' probe was constructed out of 50-μm-diam magnet wire (see Fig. 2).

A two axis, 24 element probe was constructed to measure the principle axial and azimuthal FRC magnetic field

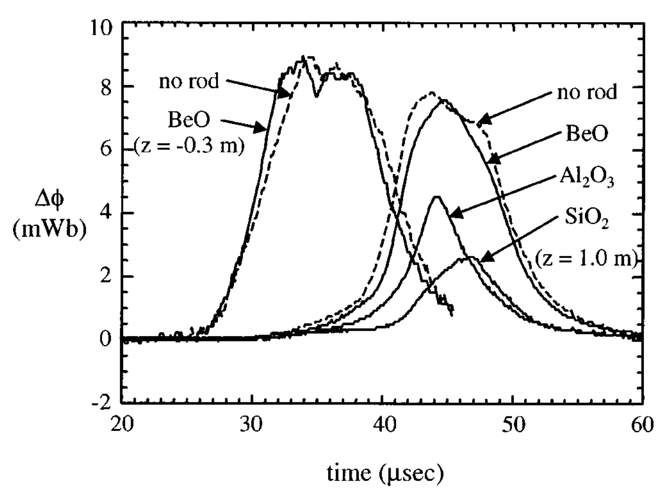

FIG. 1. Probe effect on FRC internal energy decay rate after transiting various probe materials. The excluded flux signals prior to probe transit (at $z=-0.3$ m) for all materials were similar to the case with no rod. For clarity, only the signal for BeO and no rods are shown.

Downloaded 18 Apr 2001 to 128.95.33.238. Redistribution subject to AIP copyright, see http://ojps.aip.org/rsio/rsicr.jsp

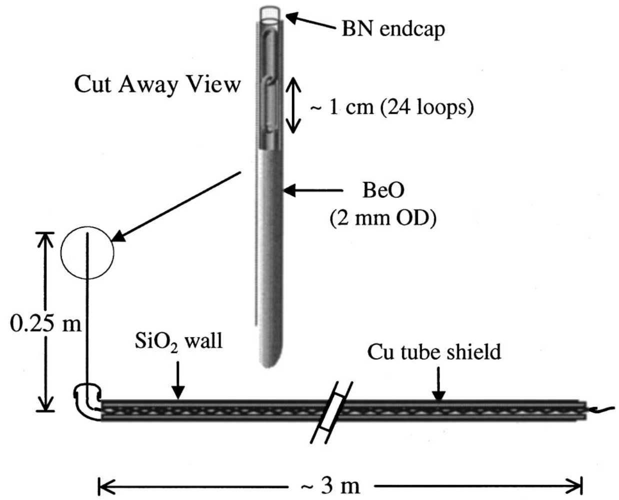

FIG. 2. Schematic of the internal magnetic probe array used in the STX experiments.

components. Each pickup loop was approximately 1.1 cm long by 0.15 cm wide and was composed of eight individual turns of the copper wire. The pickup loops were threaded together in exactly the same manner as links in a chain, and consequently, adjacent loops were nearly orthogonal. The leads to the probes ran down the length of the beryllia tube and out the lower end into a quartz tube parallel to, and resting on, the bottom of the 40-cm-diam Star Thrust Experiment (STX)[8] vacuum chamber. The beryllia tube was fixed orthogonally to this quartz tube and was positioned radially up into the STX vacuum chamber, passing through the $r=0$ axis of symmetry. The tip of the beryllia tube was capped with a small piece of boron nitride to prevent plasma entering the tube from the probe tip. The leads to each of the pickup loops were also made from the thin copper wire and were twisted with approximately ten twists per cm in order to reduce stray flux coupling. This was important since it was desired to move the location of the transverse probe array axially over several meters inside the STX vacuum chamber.

A three axis probe was also constructed by encircling each pair of orthogonal loops with loops that formed a solenoidal winding along the axis of the beryllia tube. Due to the small cross section of these loops, roughly 100 turns per probe were used. The third axis was found to be unnecessary since the probe array was used to measure a transverse rotating magnetic field (RMF),[8] and measuring the one transverse (azimuthal) component was sufficient.

Due to the lack of a winding form the probe effective cross-sectional area and direction were variable from loop to loop, but adjacent loops were found to be nearly orthogonal. The final probe calibration was carried out after the probe was installed in the chamber. Inside the flux conserving coil a very uniform axial field could be generated and provided the loop sensitivity to a known B_z. The RMF antenna consisted of two sets of coils that independently produced uniform B_x and B_y oscillatory fields (at 350 kHz). These coils were used to calibrate the individual probe's sensitivity to these fields. By using the signals from pairs of adjacent loops, the axial and azimuthal field components during a discharge could be unfolded.

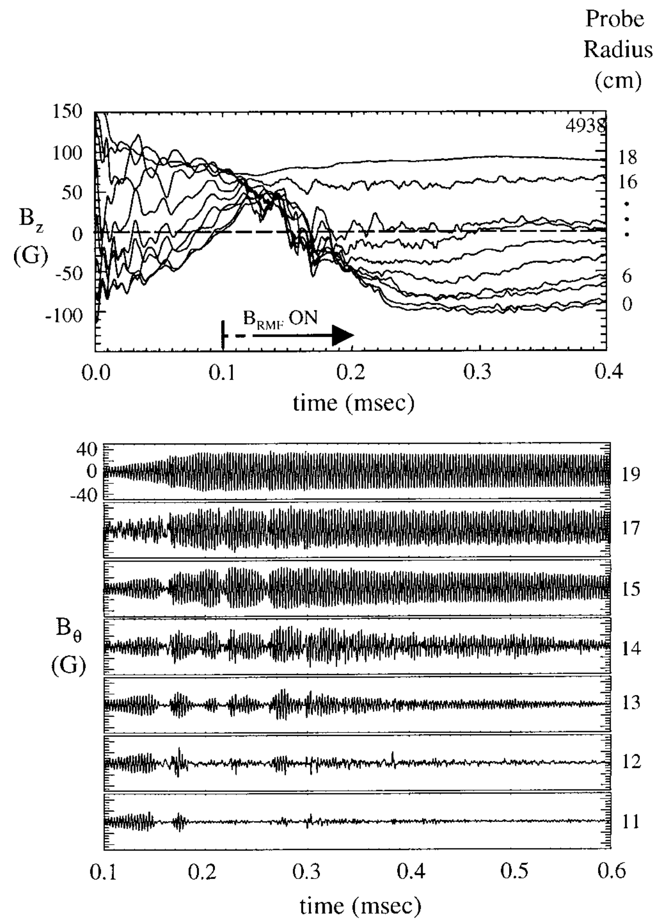

FIG. 3. Data taken from internal probe array on STX. The upper traces are the signals from axial magnetic field component from every other loop in the array. The lower traces show the transverse (θ) component of the magnetic field produced by the RMF antenna at the edge of the FRC.

Probe data from the RMF experiments on STX are shown in Fig. 3. High sensitivity and high frequency response of the probes was needed to observe the screening of the RMF by the plasma [see Fig. 3(b)]. With the probe inserted, no changes in FRC confinement or behavior were observed over the entire lifetime of the discharge (up to 1 ms). The STX plasma density and electron temperature was $5\times10^{18}\,m^{-3}$ and 60 eV, respectively. Due the preferential loss of the higher energy electrons in the sheath near the probe, it is assumed that each electron to strike the probe loses $3\,kT_e$ of energy. The power flow to the probe was thus estimated to be 8 kW. The power loss from the plasma was estimated to be 60 kW, so that the probe energy losses were not the dominant loss mechanism.

IV. PROBE ELECTRONICS

Flux penetrating the loop generates a loop voltage proportional to the change in flux. The signal from these probes is electronically integrated to provide a direct measure of the magnetic field. A schematic of the circuit used is shown in Fig. 4. It consists of a 20 microsecond integrator followed by an amplifier with a gain of 20. Such a high gain circuit is needed due to the very small size of the magnetic probes and to the need to accurately measure small changes in small fields.

Downloaded 18 Apr 2001 to 128.95.33.238. Redistribution subject to AIP copyright, see http://ojps.aip.org/rsio/rsicr.jsp

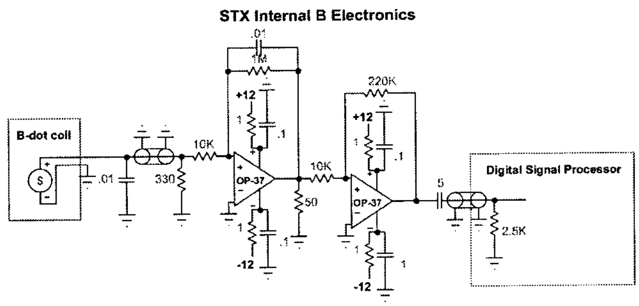

FIG. 4. Electrical schematic for the electronic integration and amplification of the internal magnetic probe signals.

The environment in which the probe operated was harsh. It was embedded in a plasma being driven by a multi megawatt rf antenna operating at several kilovolts. In this environment the probes were required to measure millivolt signals. Typical axial fields in STX have an amplitude of 100 G with a few hundred microsecond rise and fall time, while typical RMF fields have an amplitude of 25 G with a microsecond rise and fall time. At the input to the integrators, the axial fields generate peak voltages of a few millivolts, while the RMF generates peak voltages of several hundred millivolts. At the output of the amplifiers, these each produce typical maximum voltages of a few hundred millivolts. Since the digitizers used have a peak sensitivity of 2 mV per digital count, the internal probe should be able to measure STX fields down to the gauss level. In reality, signal noise limited the probe's resolution to a few gauss.

To control noise pickup the following measures were employed. The first was a tight twisting of all the probe leads over the 30 m to the screen room. This twisting keeps the effective area between the twin lead small compared to the pickup area of the probe itself. The second noise control technique involves running all the leads through a thick walled copper pipe to shield them from electrostatic noise and rapid field changes. This copper shielding extends from the base of the beryllia tube all the way back into the screen room A 10 nF capacitor was placed across the probe leads inside the screen room where the transition is made to coaxial cable. This capacitor together with the 20 Ω probe loop resistance make a low pass filter at 5 MHz, which is the Nyquist frequency of the digitizers. This filter was the limiting factor for the probe temporal response since the flux penetration of the loop was less than 50 ns.

In conclusion, an internal probe was constructed and tested in a plasma where the power density to the probe was 5 MW/m^2 with no observable effect for the discharge time of roughly 1 ms. The probe had sufficient sensitivity and time response to measure gauss level fields at MHz frequencies.

[1] M. Tuszewski, Nucl. Fusion **28**, 2033 (1988).
[2] M. Tuszewski, Rev. Sci. Instrum. **61**, 2937 (1990).
[3] K. I. Sato, Y. Osani, and T. Aizawa, Nucl. Fusion **20**, 1173 (1980).
[4] A. L. Hoffman, J. T. Slough, and D. G. Harding, Phys. Fluids **26**, 1626 (1983).
[5] K. F. McKenna, W. T. Armstrong, and R. R. Bartsch, Phys. Rev. Lett. **50**, 1787 (1983).
[6] D. E. Ashby, J. Nucl. Energy, Part C **5**, 83 (1962).
[7] J. T. Slough and A. L. Hoffman, Phys. Plasmas **6**, 253 (1999).
[8] J. T. Slough and K. E. Miller, Phys. Plasmas **7**, 1945 (2000).

Downloaded 18 Apr 2001 to 128.95.33.238. Redistribution subject to AIP copyright, see http://ojps.aip.org/rsio/rsicr.jsp